ELSEVIER

PII: S0266-3538(98)00048-7

Composites Science and Technology **58** (1998) 1827–1837
© 1998 Elsevier Science Ltd. All rights reserved
Printed in Great Britain
0266-3538/98 $—see front matter

MEASUREMENT OF *IN SITU* FIBER/MATRIX INTERFACE STRENGTH IN GRAPHITE/EPOXY COMPOSITES

Allen Yu & Vijay Gupta*

Department of Mechanical and Aerospace Engineering, University of California, Los Angeles, CA 90095, USA

(Received 25 July 1997; revised 23 December 1997; accepted 11 February 1998)

Abstract

A new experimental strategy for in situ *measurement of the fiber/matrix interface strength is presented. As-fabricated graphite/epoxy laminates with specially designed grooved islands on their front surfaces were loaded on their rear sides by a 16 to 20 ns long laser-generated pressure pulse. This compressive stress pulse, generated in-line on the rear of one of the surface islands, propagates normal to the plane of the laminate and very quickly attains a steady-state profile of approximately 130 μm after undergoing multiple scattering from individual fibers and laminates. The returning tensile wave from the sample's free surface prises the composite island off by nucleating a subsurface crack. This crack on the local scale comprises several fiber/matrix interface debonds connected by the intervening matrix. The free-surface velocity causing this damage is recorded by interferometry and related to the far-field composite-scale tensile stress by using a one-dimensional elasto-dynamic analysis. The local fiber/matrix interface stress concentration corresponding to this overall tensile stress was determined next by using a finite-element simulation that idealized the fiber distribution within the epoxy matrix to be periodic. The interface tensile strength was taken as the sum of this stress and the compressive residual stress at the same location, which in turn, was estimated by yet another analysis based on the finite-element procedure. For a graphite/epoxy laminate fabricated from a unidirectional Hercules AS4 graphite fiber tapes pre-impregnated with 450 k cure Hercules 3502 thermosetting epoxy resin, an average fiber/matrix interface strength of 210 MPa was estimated.* © *1998 Elsevier Science Ltd. All rights reserved*

Keywords: fiber/matrix interface strength, graphite/epoxy composites, stress waves, optical interferometry

1 INTRODUCTION

Measurement and control of fiber/matrix interface strength is important for developing tailored composite microstructures where enhanced toughness is achieved by promoting controlled decohesions at fiber/matrix interfaces. The overall strength and stiffness of such composites are also dependent on the mechanical properties of the interfacial region since this occupies a rather large volume fraction within the composite microstructure. Hence, the development of such tailored composites requires a strategy to measure the intrinsic tensile strength and toughness of fiber/matrix interfaces. The emphasis here is on the measurement of the intrinsic properties because these depend solely on the structure and chemistry of the interfacial region and are relatively free from the large plasticity effects that usually accompany the interface decohesion process. Only a few experimental procedures can accomplish this task and that, too, on planar interface geometries.[1,2] In contrast, a number of methods are available that can directly or indirectly measure the *overall* strength or *total* toughness of interfaces (defined as the sum of the fundamental or the intrinsic interface energy and the dissipative energy components in the interfacial region that accompany interface crack growth). Such measurement depends upon many extrinsic parameters such as specimen geometry, loading rate, temperature, surface roughness, interface flaws, and the local tensile to shear stress ratios. Each of these extrinsic parameters influence the inelastic dissipative mechanisms in the vicinity of the crack tip, and consequently, the fracture resistance or the total toughness of the interface becomes larger than the basic adhesion (measured either in terms of the intrinsic tensile strength or fundamental fracture energy of the interface) by two orders of magnitude and higher.[3]

While both these parameters are of interest to the composites research community for the developing of design rules and predicting failures, for the purposes of manufacturing tailored composites, as is the focus here, we concentrate only on the measurement of the intrinsic fiber/matrix interface tensile strength in as-fabricated composite panels. To accomplish this task, a new experimental procedure based on a recently developed technology of laser-generated stress pulses is presented. Regardless of the type of composite, such measurements have never been accomplished before.

*To whom correspondence should be addressed.

Boeing Ex. 1032, p. 1 of 15
Boeing v. Regents Univ. Cal.

Previously, the tensile strengths of interfaces formed by a variety of metal, ceramic, and dielectric films on a number of engineering substrates were measured under ambient conditions by using laser-generated stress pulses.[4–7] As discussed later, this so-called laser-spallation experiment is capable of measuring the intrinsic tensile strength of flaw-free interfaces. While the technique can in principle be applied to any type of composite, whether metal-, polymer- or ceramic-matrix-based, we shall focus here only on the Hercules AS4/3502 composites to demonstrate its feasibility.

A review of the presently available methods to characterize fiber/matrix interfaces is presented first, followed by a discussion of the basic laser-spallation test methodology. The sample preparation and the new procedure for examining the *in situ* interface strength are discussed next. The paper ends with a comparison between this new technique and others in the literature.

2 LITERATURE REVIEW

Three commonly used methods to measure the fiber/matrix interface strength are the fiber pull out test, the micro-indentation test, and the fragmentation test. In the pull-out test, a fiber embedded in a matrix is directly pulled at its free protruding ends until the fiber debonds from the matrix. The pull-out experiment is thought to possess some of the characteristics found in the wake of a propagating matrix crack where the bridging fibers break and pull-out from the matrix. Variations to this test can be found essentially in the matrix portion, where the fiber may be pulled out from either a matrix block, a disc or a droplet.[8] In the fragmentation test,[9] a standard dog bone-shaped matrix specimen with a single embedded fiber is pulled until the fiber fractures into segments of some critical length. The de-fragmentation process terminates when the correspondingly smaller interfaces can no longer transfer sufficient loads across the interface to cause further fiber breakage. A shear-lag analysis on the fragments is typically done to quantify the interface shear strength. In the micro-indentation test,[10] a sample is made from a thin cross-section of a composite where each fiber is individually pushed out with a micro-indentor. In contrast to the pull-out and fragmentation tests, the micro-indentation technique is an in situ test. As-manufactured composites samples can be used, and thus, the effects of various processing variables and servicing conditions, including fatigue and environmental exposure, on the fiber/matrix interface strength can be evaluated. A critical review of these techniques can also be found in Ref. 11. The main difficulty with all three techniques lies in the complex post-experimental analysis needed to determine the local stresses responsible for causing the fiber/matrix debond. Such analyses typically involve an evaluation of complex local stresses, including a large undetermined zone of local plasticity, near the interfacial region. Backing out the local fiber/matrix interface stress at the onset of failure thus becomes an exercise dependent upon a large number of assumed model variables.

3 THE LASER-SPALLATION TECHNIQUE FOR MEASURING THE TENSILE STRENGTH OF THIN FILM INTERFACES

In the experiment (Fig. 1) developed previously to measure the tensile strength of thin film interfaces (films up to 100 μm thick), a 2.5 nanosecond (ns) long Nd:YAG laser pulse is made to impinge over a 3 mm-diameter area on a 0.3 μm-thick aluminum film which is sandwiched between the back surface of a substrate disc and a 5 to 10 μm thick layer of solid water glass. This layer is provided as a liquid solution of sodium silicate, which dehydrates within a few minutes when exposed to air, and leaves behind a continuous layer of solid SiO_2, covering the aluminum film. The melting-induced expansion of aluminum under confinement generates a compressive stress pulse with one nanosecond rise-time directed towards the test coating which is deposited on the substrate's front surface. The compressive stress wave reflects into a tensile pulse from the coating's free surface and leads to its spallation (complete removal) at a sufficiently high amplitude. The critical stress at the interface is calculated by measuring the transient displacement history of the coating's free surface (induced during pulse reflection) by using an optical interferometer (shown towards the right in Fig. 1) which is capable of recording fringes from even optically rough surfaces and with a resolution of only 0.2 ns in the single shot mode. For a coating of density ρ, thickness h, and longitudinal wave velocity c, the interface stress σ is calculable from the measured transient velocity $v(t)$ using

$$\sigma(h, t) = \frac{1}{2}\rho c\left[v(t+\frac{h}{c}) - v(t-\frac{h}{c})\right] \quad (1)$$

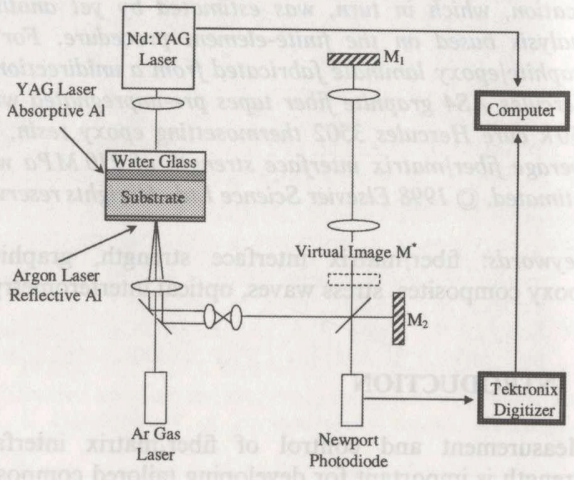


Fig. 1. A schematic of the basic laser-spallation setup along with that of a wide angle interferometer.

Boeing Ex. 1032, p. 2 of 15
Boeing v. Regents Univ. Cal.

The major advantage of this technique over its counterparts is in its ability to provide a fundamental measure of the bond strength, since interface decohesion is achieved at a relatively high strain rate ($10^7\,s^{-1}$) during which all inelastic dislocation-related processes are essentially suppressed, and the measured values relate directly to the atomic structure and chemistry of the interfacial region. Additionally, the short rise time of the stress pulse is able to invoke a rather local response of the interface such that minute changes in the atomic structure and chemistry are reflected directly in the measured overall strength values. This was recently demonstrated on interfaces between sputter-deposited polycrystalline niobium coatings and sapphire substrates[12], where structural changes brought about by different heat treatment cycles and different thicknesses of the intervening chromium and antimony layers were shown to directly affect the tensile strength of the interface.

The aim of the present work was to tailor that procedure for the *in situ* testing of cylindrical fiber/matrix interfaces in as-fabricated graphite/epoxy composites. Although the basic procedure essentially remains the same, several modifications to the sample preparation and interface stress quantification were necessary to accommodate testing of the non-planar interface geometry. Such changes and their rationale are discussed next.

4 MODIFICATIONS TO THE LASER-SPALLATION TECHNIQUE FOR TESTING COMPOSITES

4.1 Sample preparation

The graphite–epoxy composite samples tested in this investigation were fabricated from commercially available unidirectional Hercules AS4 graphite fiber tapes pre-impregnated with 450-K cure Hercules 3502 thermosetting epoxy resin. The tapes were laid to form 8-ply laminates totaling approximately 1 mm thick.

The as-manufactured 1 mm thick composite panel was diced into 25 mm × 12.5 mm rectangular plates with a diamond saw. Since the epoxy of the composite near the sample surface was found to vaporize easily upon absorption of the YAG laser pulse, use of laser-absorbing A1 film was deemed unnecessary for the present experiments. However, a 5 to 10 μm-thick water glass layer was still used on the surface for constraining the vaporizing material for generating sufficient stress pulse amplitudes.

The backside of the composite sample was loaded in the same fashion as the thin film experiment discussed earlier. Since the stress pulse wavelength was long, the peak tensile stress caused by the reflected wave occurred at a relatively deep subsurface location. At a critical tensile stress amplitude, subsurface cracks spanning several fiber/matrix nucleated and coalesced without forming a free spall (i.e. complete removal of the material). In fact, the latter was found to happen at a much higher stress level since the nucleated sub-surface crack had to break through the overlying fiber weaves at the edges of the stressed area in order to form a free spall. The onset of damage is of obvious interest to the present work; however, because of the cracks' typical small dimension and deep subsurface location, it could not be easily detected by any of the currently available non-destructive evaluation methods. In order to tackle this problem, a novel sample geometry was designed. Surface grooves approximately 400 μm deep were cut on the front surface (opposite to the one covered by the water glass layer) of the sample by using a diamond saw, in order to create square islands of approximately 2.5 mm in length. Figure 2 shows a schematic of the surface cross-section; Fig. 3 provides a close perspective view of one of the islands and its associated grooves as seen under a scanning electron microscope.

The island dimensions were designed in order to attain planar stress wave conditions at the spallation site. Even as the ratio of the laser spot size ($\approx$3 mm) to propagation distance ($\approx$1 mm) remains around 3 to ensure the planar wave front reaches the fracture site, surface edges introduced by the grooving process still caused some lateral wave fringing effects. The macroscale stress state changes from one of uniaxial strain

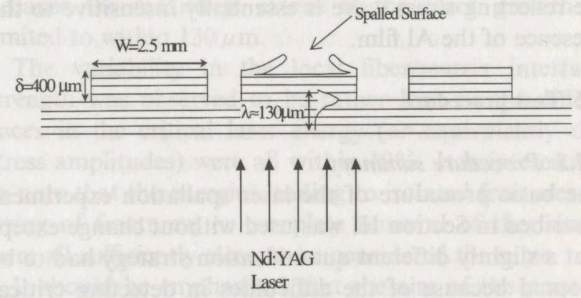


Fig. 2. A schematic showing the cross-section through the grooved surface of the sample.

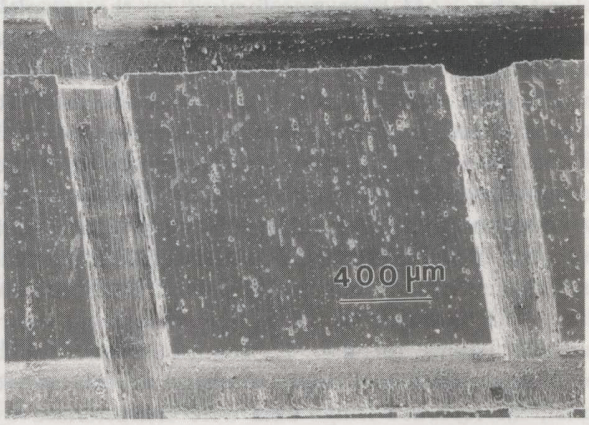


Fig. 3. A close perspective view of one of the island and its associated grooves as observed in a scanning electron microscope.

Boeing Ex. 1032, p. 3 of 15
Boeing v. Regents Univ. Cal.

within the island's central region to that of uniaxial stress near its edges (as a result of the traction-free boundary conditions), and the stress correspondingly decreases slightly from the middle to the edge of the island. The maximum extent of the edge effects are expected to be well within one wavelength of the loading stress wave, which for the present case is of the order of 130 μm. Thus, by maintaining the island width ($\approx$2500 μm) to be much larger than the wavelength λ, uniaxial strain conditions are attained over 90% of the island area. These considerations have also been used previously to analyze the stress-state in Hopkinson Bar experiments. It is noteworthy that because of this constraint, exactly the same stress state is expected to develop in an ungrooved sample at the same subsurface location. As shown later, this drop of stress towards the island's edges encourages the damage to initiate from the interior and not from the edges. This, coupled with the additional fact that the maximal amount of damage is expected to grow only to the order of the wavelength λ (see next section), would render the effect of any defects introduced by the surface cutting process to be negligible.

To improve the reflectivity to the Argon laser beam even while using the wide-angle interferometer, a 0.1 μm-thick Al reflecting coating was deposited on top of the grooved surface. Since the thickness of the Al layer is much smaller than the length of the stress pulse, the reflecting stress wave is essentially insensitive to the presence of the Al film.

4.2 Test procedure

4.2.1 Procedure summary

The basic procedure of the laser spallation experiment described in Section III was used without change except that a slightly different quantification strategy had to be adopted because of the difficulties in detecting critical spallation in composites.[13] Also, an additional numerical simulation was necessary to recover the stress-state at the local fiber/matrix interface.

First, the YAG laser was focused on the sample's back surface in-line with one of the square islands. The laminate was subjected to successively higher laser energies until free-surface spallation was observed. To avoid any fatigue effects, the laser heating spot was aligned with a new island after each sub-threshold loading. The depth of the spalled spot was determined by using an Alpha Step 200 profilometer that had a resolution of few angstroms. For each test, the transient displacement experienced by the central region of the island was recorded by using the wide-angle interferometer shown in Fig. 1. Because of the rough composite surface and high frequency content of the signal, the recorded fringe data were characterized by noise and varying amplitudes. To unambiguously reduce this fringe data to the surface velocity, the velocity profile was independently recorded by using a linear velocity interferometer.[14] The resulting critical free surface velocity was converted to the tensile stress at depth h by using eqn (1). This calculated critical stress can only be considered as an overall effective strength since the length of the final tensile wave is at least 20 times the diameter of the individual fibers. Note that the initial pulse, which is of the order of 60 μm in extent, very quickly attains a steady-state profile after undergoing multiple reflections from interply and fiber/matrix interfaces during its propagation toward the free surface. To recover the desired local fiber/matrix interface strength, a finite element cell model was constructed with the measured effective stress as an input. A brief description of each stage of the quantification procedure is provided later.

4.2.2 Determination of the threshold laser energy

For determining the threshold stress, the energy of the laser pulse was increased while keeping the laser in-line with the island on the rear side and constant at about 3 mm. If no visual spallation was observed, the laser beam was aligned with another unloaded island to rule out the effects of fatigue loading.

At the threshold laser energy, corresponding to the formation of a critical crack at a subsurface location, the entire coupon above that plane was completely spalled off. However, at times, because of the variation in the local microstructure, only a part of island was completely removed. This can be seen in a scanning electron micrograph of the failed coupon in Fig. 4, where the spalled spot is marked by an arrow.

There is always a question of whether any edge defects that might have been introduced during the surface grooving process could have caused premature spallation in the grooved samples. The following observations seem to suggest not. First, in all the samples, spallation was observed to initiate from the middle, not the edges, of the coupons. This can be seen in Fig. 4, where even though the central portion of the island has completely spalled off, the crack (shown by two arrows at the bottom of the figure) causing this failure seems to

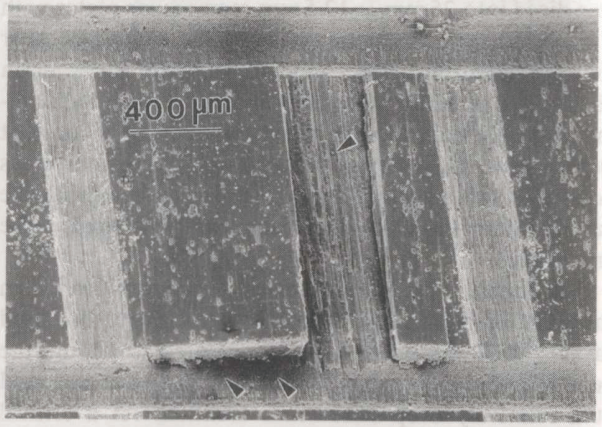


Fig. 4. Scanning electron micrograph of a critically spalled island. The spalled surface is marked by an arrow.

Boeing Ex. 1032, p. 4 of 15
Boeing v. Regents Univ. Cal.

have stopped just prior to reaching the island's left edge. This initially surprising observation is actually expected when one realizes that the stress, as mentioned earlier, varies from a uniaxial strain to a uniaxial stress state from the center to the edge of the coupon. Second, little variation in the critical spallation energy was observed (within 8%) from island to island on a given sample. If edge defects were to control the island spallation, one would expect to see a much larger strength variation. Finally, any edge defect can only grow to a maximum of about 130 μm ($=\lambda$) into the sample since the crack propagation speed has to be bounded by the highest Rayleigh wave velocity ($\approx$one half of the P-Wave speed) within the bi-material pair caused by energetic arguments. Therefore, since the island's width (2500 μm) is much larger than the stress wavelength, such cracks cannot lead to the spallation of the coupon.

Because the stress state in an ungrooved sample just a wavelength away from the sample's edge is expected to be the same as in the island's interior, the critical energy required to cause subsurface crack formation in a grooved and an ungrooved sample should be close. As expected, though a free surface rupture was not observed from an edge shot in an ungrooved sample, a high magnification view of the sample's edge revealed the formation of a crack of several fiber/matrix diameters. Figure 5 shows a scanning electron micrograph of the sample's edge and the formation of the aforesaid crack. Apparently, even though the stress level is somewhat lower at the edges because of the uniaxial stress state, the nucleated subsurface crack away from the edge appears to have sufficient energy to grow and exit from the sample's lateral edge. This is not surprising, since the expected zone over which the stress drops slightly is limited. Encouraged by the earlier discussed observations, a rather involved effort was undertaken where the sample's free edge was searched for initiation of isolated fiber/matrix debonds at threshold conditions. Figure 6 shows one such example. It is interesting to note that the difference of the threshold energies between the grooved and ungrooved samples was well

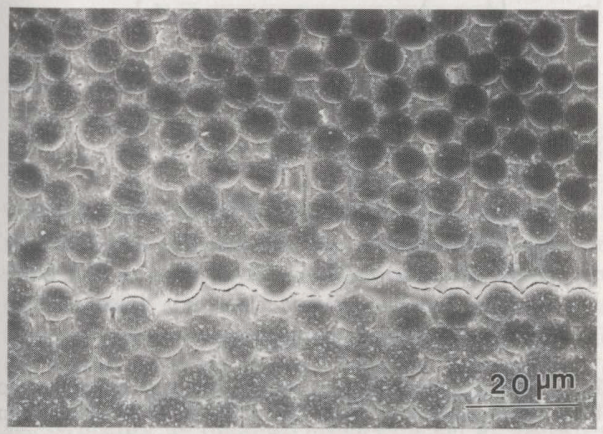


Fig. 5. A collection of local fiber/matrix interface debonds as observed on the lateral edge of an ungrooved sample.

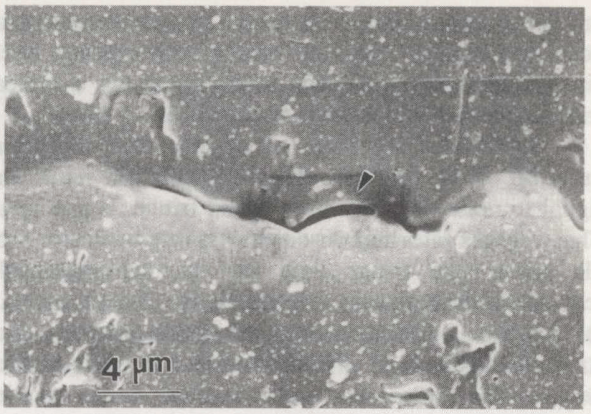


Fig. 6. A scanning electron micrograph showing isolated fiber/matrix interface debonds.

within the experimental error (of about 5%) inherent to the laser spallation procedure.

Although the exact sequence of events leading to the formation of the crack shown in Fig. 5 could not be captured, two scenarios are possible. First, many interfaces fail simultaneously and then grow laterally to coalesce. Second, the weakest of the interfaces fail and grow laterally to induce failure in neighboring interface. However, since failures involving multiple interface fractures occurred over a 2 mm length, clearly this could not have occurred by fracturing of only one interface because the maximum extent of the crack growth is limited to within 130 μm.

The variability in the local fiber/matrix interface strength was observed to be rather low, as the differences in the critical laser energy (or equivalently the stress amplitudes) were all within 10%. It is interesting to note that the energies leading to isolated fractures, a string of fractures, or complete removal of the island were all sufficiently close to be considered the same.

It should be emphasized that the aim of the present investigation is to quantify only the nucleation of interface cracks. Since the laser energy can only be incremented by a certain minimum unit, the present experiment is unable to discriminate crack nucleation vs propagation events that occur during this increment range. This, however, is not a problem since this minimum increment of 5% of the laser fluence is well within the experimental error and also the observed material strength variation of 8 to 10%. The stress causing damage initiation at the interface is a direct measure of the fiber/matrix bond strength. The method to calculate this stress from the recorded threshold laser fluence is discussed next.

4.2.3 Determination of the free surface velocity using interferometry

The wide angle interferometer shown in Fig. 1 was used for recording the free surface velocities from the central region of the island, which as stated before was covered with a thin aluminum film to improve reflectivity. The

Boeing Ex. 1032, p. 5 of 15
Boeing v. Regents Univ. Cal.

interferometer design is somewhat similar to that proposed by Amery[15] and its details have already been given earlier. The solid line in Fig. 7 shows a typical fringe record obtained from the surface.

As a result of the rather sharp rise time and short duration of the signal in the laser spallation setup, the signal to noise ratio of the recorded fringes is not ideal. This requires information on the expected velocity profile before the fringe data can be unambiguously reduced to the transient velocity profile. To get such an information, a linear velocity interferometer was constructed. In this type of interferometer the delay length between the two optical paths is made much smaller than the rise time of the velocity pulse so that the photodetector output is directly proportional to the free surface velocity.

In this modified interferometer (shown in Fig. 8), the delay leg of two lenses and one mirror of the interferometer shown in Fig. 1 is replaced by a de-ionized water-filled etalon with a mirror on one end. The etalon was constructed of a plexiglas tube of 50.8 mm inner diameter and about 175 mm in length, capped at the ends by fused silica windows of 12.5 mm thickness. The fused silica window on the left end had a 5 μm thick layer of aluminum deposited on the outside to act as mirror M2 as shown in Fig. 8. Once again, the apparent position of M2 (M2*) and M1 are equidistant from the beam splitter BS. As a result of the higher index of refraction of water compared to air (1.3 compared to 1), the actual optical position of M2 is at M2,** yet this is much less than the actual optical position of M2 in Fig. 1. This reduction in actual optical distance traveled between the two interferometers reduces the time lag between the delayed beam and the signal beam to approximately 0.67 ns. Since the expected rise time of the velocity pulse recorded in this experiment is appreciably

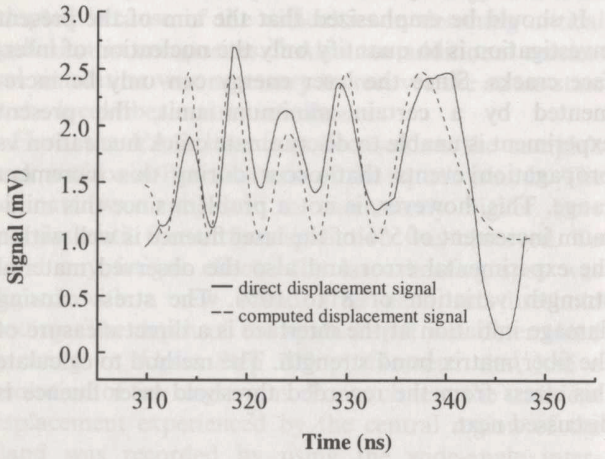


Fig. 7. Fringe records used for the calculation of the interface strength. The one shown by solid line was measured using the displacement interferometer of Fig. 1, whereas the one in broken line is the closest fit to the direct one after adjusting the amplitude of the velocity-fringe recorded by using the linear velocity interferometer of Fig. 8. Both fringe record correspond to the critical spallation event.

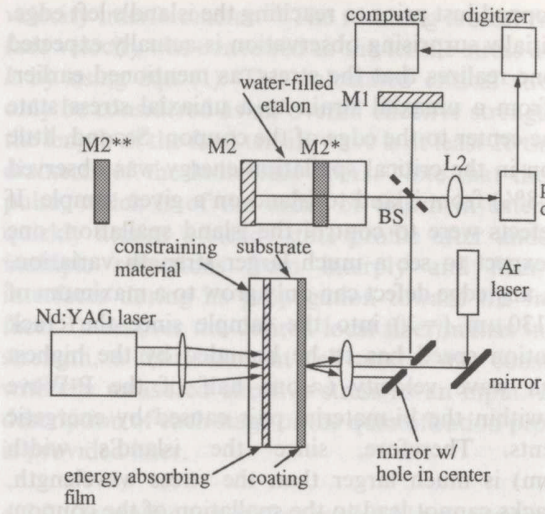


Fig. 8. A schematic of the linear velocity interferometer.

larger than 0.67 ns, the photodetector output is directly proportional to the transient surface velocity. Because the linear interferometer provides information proportional to the actual velocity, the amplitude of the velocity remains undefined. A best fit curve to the velocity profile was obtained and integrated to obtain the closest match between the calculated and recorded displacement fringes by varying the velocity amplitude. The dashed line in Fig. 7 corresponds to the calculated displacement fringe record obtained from the velocity interferometer while the solid line corresponds to the measured signal obtained from the original displacement interferometer. The velocity profile that resulted in the best fit is shown in Fig. 9. How this information is used to determine the local fiber/matrix interface strength is discussed next.

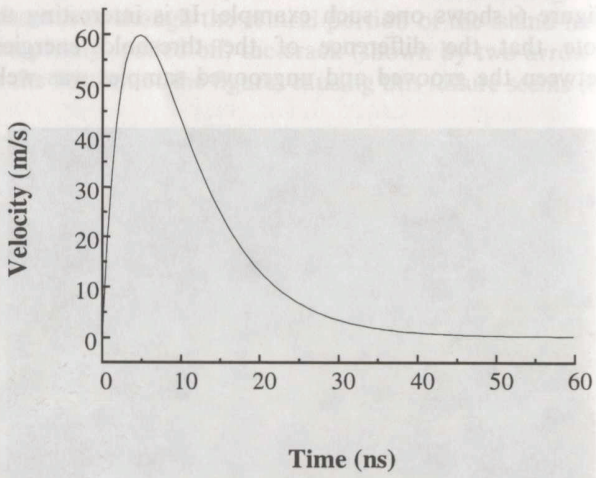


Fig. 9. The assumed velocity profile that was integrated to obtain the displacement fringe record shown by broken line in Fig. 7. The amplitude of the velocity pulse was adjusted until a close fit to the directly recorded displacement fringe record (shown by solid line) was obtained.

Boeing Ex. 1032, p. 6 of 15
Boeing v. Regents Univ. Cal.

Table 1. Material constants used in the simulations[17]

	E_L (GPa)	E_T (GPa)	μ_L (GPa)	$^*\mu_T$ (GPa)	ν_{LT}	ν_T	ρ (kg m^{-3})	α_L (10^{-6} °C^{-1})	α_T (10^{-6} °C^{-1})
Hercules AS4 fiber	235	14	28	5.5	0.20	0.25	1,790	−0.36	18
Hercules 3501-6 matrix	$E(T)$	$E(T)$	1.6	1.6	0.34	0.34	1,260	$\alpha(T)$	$\alpha(T)$
Composite properties	147.5	10.5	18.01	4.02	0.25	0.28	1,589	—	—

$E(T) = -2.11\times10^{-5}\,T\,(°C) + 4.812$; $\alpha(T) = 0.122\,T\,(°C) + 38.3$; where T is the temperature in Celsius. $^*\mu_T = E_T/2(1+\nu_T)$.

4.2.4 Interface stress calculation

Because of multiple wave scattering with the fibers, the originally sharp stress pulse of 16 ns duration very quickly attains a wavelength much larger than the interfiber spacing. This can be seen from the velocity profile recorded from the composite's free surface, showing a temporal extent of almost 40 ns, which for the graphite/epoxy laminate corresponds to a wavelength of roughly 130 μm. This is clearly several times the fiber diameter of 8 μm. After accomplishing a steady-state profile, the wave then travels without much further dissipation as the conditions of plane wave propagation are maintained all the way until the reflected tensile wave pries off a collection of fiber/matrix interfaces at a sub-surface location. In addition, because the loading is accomplished at a strain rate of almost $10^7\,s^{-1}$, all inelastic deformations in the stressed continuum and those accompanying the fiber/matrix decohesion process are largely suppressed. Therefore, the stress-state in the immediate vicinity of the fracture site can be determined by considering the composite to be homogeneous and elastic, and using the one-dimensional elasto-dynamic equation for the uniaxial strain condition:

$$\frac{\partial^2 u}{\partial x^2} = \frac{1}{c^2}\frac{\partial^2 u}{\partial t^2} \tag{2}$$

where $c^2 = \frac{C_{22}}{\rho}$ and ρ is the medium's density, u is the displacement and t is time. C_{22} is calculated from the composite properties listed in Table 1[16] using,

$$C_{22} = \frac{(1-\nu_{LT}\nu_{TL})E_T}{(1+\nu_T)(1-\nu_T-2\nu_{LT}\nu_{TL})} \tag{3}$$

where, owing to the symmetry of the stiffness matrix,

$$\frac{\nu_{LT}}{E_L} = \frac{\nu_{TL}}{E_T} \tag{4}$$

where L and T refer to directions along and normal to the fiber axis, respectively. The solution to this equation subjected to traction-free conditions at the island's free surface using the measured free-surface velocity as an input is rather straightforward and leads to eqn (1) for the tensile stress at a depth h from the free surface. For a typical velocity profile of Figs 9 and 10 shows the stress history as obtained using eqn (1) at an experimentally determined (using the Alpha Step 200 Profilometer) spallation depth h of 63 μm. As expected, the stress is compressive during the onward journey of the wave and turns tensile some time later as a result of the arrival of the reflected wave. The peak of the tensile front is taken as the overall continuum-scale stress causing the local fiber/matrix interface debonds. A finite element procedure to extract the local interface stress-state is discussed next.

4.2.5 Quasi-static finite element analysis for calculation of the interface stress concentration factors

The calculation of the local interface stress-state was accomplished by using a quasi-static finite element analysis that considered only a periodic square arrangement of the fibers. This minimized the simulation effort significantly as the discretized region could be reduced to a single fiber surrounded by a block of matrix.

A quasi-static model is justified since it is the static effects that dominate the dynamic field when the wavelength, λ, is much greater than the size of the local inhomogeneity. The stress concentration, therefore, will arise mainly because of the mismatch in the elastic moduli rather than the mismatch in the densities.[17]

An exact finite element analysis that models all the details of the composite microstructure comprising of randomly distributed fibers over a 3 mm × 1 mm cross-section is rather cumbersome and unnecessary as the stress state of interest as determined from the periodic cell model turns out to be quite insensitive to the volume fraction of the fibers (see Fig. 12). In addition, it has been already shown, although not rigorously, that the effective stiffness of a composite is insensitive to the precise local fiber distributions in random microstructures.[18] Finally, the observed low variability in the local fiber/matrix interface strength mentioned earlier

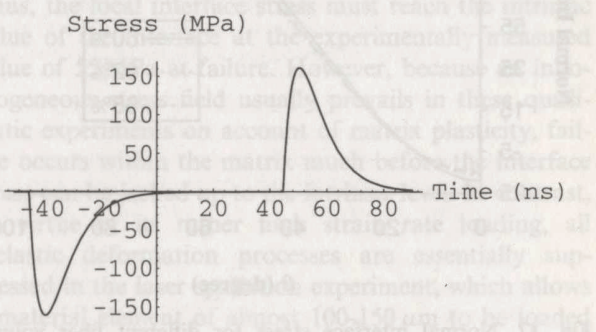


Fig. 10. The stress history at the base of the spallation crater of depth 63 μm.

Boeing Ex. 1032, p. 7 of 15
Boeing v. Regents Univ. Cal.

demonstrates, at least in an average sense, a certain insensitivity of the strength to the local random fiber distribution. It is noteworthy that the problem could have been solved by using the elegant volume integral method developed by Mal and coworkers,[19] with due consideration to local fiber distribution and without the need to consider the far-field fibers and specimen geometry, but the amount of computation needed was comparable to that in the present simulation. In addition, the residual stress calculations were easier to implement numerically. Thus, because of its familiarity and straightforwardness, the simulations were performed using a finite element-based procedure.

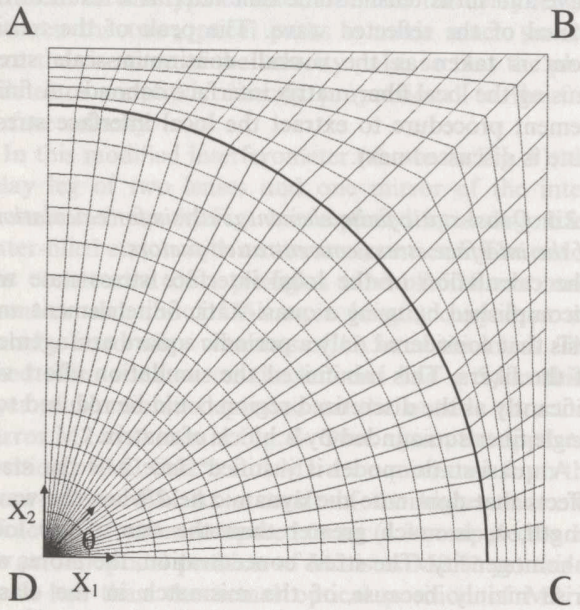


Fig. 11. The unit cell used to model the periodic square array of the fibers within the epoxy matrix for the purpose of calculating the interface stress concentrations.

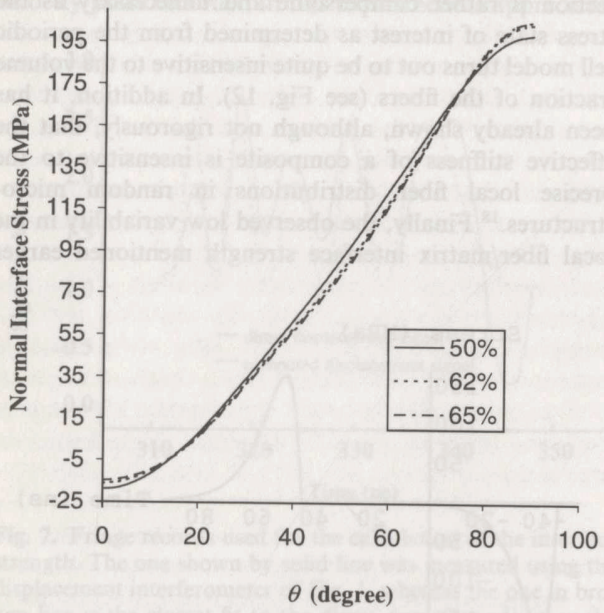


Fig. 12. Normal interface stress for different fiber volume fractions as a function of θ (in degrees) measured counterclockwise to the X_1 axis shown in Fig. 11.

A periodic square fiber-packing array with volume fraction of 62% is thus assumed, and the region of interest is reduced, via periodicity arguments, to a single fiber surrounded by a block of matrix material.[20] The analyzed unit cell is shown in Fig. 11. The boundary conditions are applied so as to maintain stress equilibrium and deformation compatibility with the neighboring cells in the periodic repeating system by constraining the lateral cell edges from warping, *viz.*,

On edge AD: $u_1 = 0$, $t_2 = 0$;
on DC: $u_2 = 0$, $t_1 = 0$;
on AB: u_2 is constrained to be uniform, $\int_{AB} t_1 dl = 0$,

$$\frac{1}{L_{AB}} \int_{AB} t_2 dl = 150 \text{ MPa}$$

(measured composite-scale stress); and

on BC: u_1 is constrained to be uniform, $\int_{BC} t_1 dl = 0$, $\int_{BC} t_2 dl = 0$.

In this equation, t_i denote tractions and u_i the displacements along the coordinate directions shown in Fig. 11, and L_{AB} the length of edge AB. All calculations were done on ANSYS[21], using the Plane42 element under plane strain conditions with the in-plane material properties given in Table 1.

In previous research dealing with testing of thin films the residual stress normal to the interface in the film thickness direction was essentially zero because of the rather small thickness of the film. Thus, the measured critical stress for decohesion could be taken directly as a measure of the interface tensile strength. The situation for the composite samples tested here is different as a result of the existence of non-planar interfaces. Any tensile residual stress generated would work to debond the interface. Consequently, the thermal residual stresses produced at the interface need to be added to the local stresses calculated from the FEM model discussed earlier to obtain the intrinsic interface strength. A simulation leading to such stresses in the vicinity of the interface is discussed next.

4.2.6 Thermal residual stress calculations

Development of the residual stresses in composite is a complex phenomenon as it depends upon a number of parameters beside the mismatch in the thermal expansion coefficients, such as the resin viscosity, curing history, and moisture, to name a few.[22–24] Despite the physical complexity, a number of research studies[25–29] have concluded that for graphite/epoxy composites an analysis based on temperature-dependent elastic property suffices for determining such stresses. For the present purpose, we will follow this thermo-elastic approach without incorporating the moisture-induced stresses since all experiments were performed in a relatively arid, laboratory environment. The fiber distribution was

Boeing Ex. 1032, p. 8 of 15
Boeing v. Regents Univ. Cal.

assumed periodic and the same cell from the stress analysis was used. A transient analysis that integrated the effects of the temperature-dependent properties over the entire cooling process (linearly from 180°C to 20°C) was then carried out with the same boundary conditions used earlier for the wave loading problem except that on the edge AB, the traction-free condition was now imposed, *viz.*,

$$\int_{AB} t_2 \mathrm{d}l = 0$$

5 RESULTS

A typical displacement interferometer signal of a composite sample undergoing critical spallation is shown by the solid line in Fig. 7. Figure 9 shows the free surface velocity associated with this displacement fringe record obtained from the procedure described earlier. Using the elasto-dynamic and homogenization assumptions described in the previous section, the stress history at the measured crack depth was obtained and illustrated in Fig. 10. The material properties used in the computation are shown in Table 1. As can be clearly seen, the fracture plane (collection of several fiber/matrix interfaces) at 63 μm from the free surface is first subjected to a compressive then a tensile stress from the passing and reflected wave. For this particular signal, the microstructure comprising of several interfaces was subjected to a peak stress of 151 MPa on the continuum-scale. The results for three other critical spallation events were 144 MPa, 146 MPa and 158 MPa, with an average value of 150 MPa. Using this average value as the far-field stress, the finite element calculations for the local, normal interface stress for various volume fractions were carried out. In agreement with results obtained by others, (e.g. see King and Adams[30]), the maximum stress at the interface (Fig. 12) changed only slightly over a rather large fiber volume fraction range, 50 to 65%. In Fig. 12, θ is the angle in degrees measured counterclockwise from the X_1 axis shown in Fig. 11. A peak value of 204 MPa was obtained for the largest tensile stress normal to the interface created by the returning tensile wave. Next, the thermo-elastic analysis on a quarter sub-unit cell was implemented, and the distribution of normal residual stresses at the interface as a function of θ is shown in Fig. 13. Once again θ is measured in degrees counterclockwise from the X_1 axis shown in Fig. 11. It was found that while the principal residual stresses in the matrix near the interface can reach in the tens of MPa range, the radial stress component remains relatively small throughout the perimeter of the fiber. This agrees well with the common observation of radial matrix cracking in composites possessing a matrix of a higher thermal expansion coefficient and reasonably strong fiber/matrix interfaces.[30] Since the maximum residual compressive stress developed is approximately equal to 10 MPa, we conclude

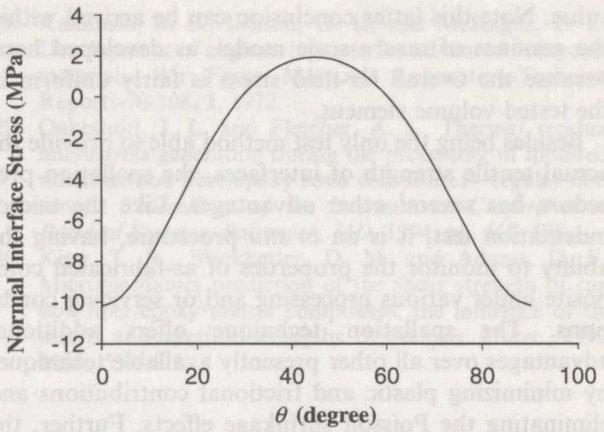


Fig. 13. Distribution of the normal residual stress as a function of θ (in degrees) measured counterclockwise to the X_1 axis shown in Fig. 11.

that the measured average fiber/matrix interface strength in as-fabricated unidirectional Hercules AS4 graphite fiber/3502 thermosetting epoxy resin composites is 214 MPa.

6 CONCLUSION AND DISCUSSION

A new experimental strategy for in situ measurement of the fiber/matrix interface strength was presented. Cylindrical fiber/matrix interfaces were loaded in as-fabricated Hercules AS4 graphite fiber/3502 thermosetting epoxy resin laminates by using a laser-generated stress pulse. The critical de-cohesion events were carefully recorded by microscopy and the local stress nucleating this damage was evaluated using a finite element simulation with the optically-recorded free surface velocity of the sample as input. The variation in the tensile strength was rather limited and an average value of 214 MPa was estimated.

It is interesting to note that the usually quoted static transverse tensile strength of AS4/3502 composite is about 55 MPa, which is quite different from the value reported here. This value should be considered as an overall strength value, far away from the local fiber/matrix interface, in the presence of matrix plasticity. Thus, the local interface stress must reach the intrinsic value of the interface at the experimentally measured value of 55 MPa at failure. However, because an inhomogeneous stress field usually prevails in these quasi-static experiments on account of matrix plasticity, failure occurs within the matrix much before the interface stress can be jacked up to the intrinsic level. In contrast, by virtue of its rather high strain rate loading, all inelastic deformation processes are essentially suppressed in the laser spallation experiment, which allows a material element of almost 100-150 μm to be loaded uniformly. Thus, the failure occurs at the weakest link with the measured number approaching the intrinsic

Boeing Ex. 1032, p. 9 of 15
Boeing v. Regents Univ. Cal.

value. Note this latter conclusion can be arrived within the confines of macro-scale model, as developed here, because the overall far-field stress is fairly uniform in the tested volume element.

Besides being the only test method able to provide the actual tensile strength of interfaces, the spallation procedure has several other advantages. Like the micro-indentation test, it is an *in situ* procedure, having the ability to monitor the properties of as-fabricated composite under various processing and/or servicing conditions. The spallation technique offers additional advantages over all other presently available techniques by minimizing plastic and frictional contributions and eliminating the Poisson shrinkage effects. Further, the technique presented here is the only one that provides a measure of the normal stress required to decohere the fiber/matrix interface. This is important because the tensile strength should constitute a more fundamental failure criterion than shear strength since at the microscopic scale it is only the local tensile stress that can cause debonding and failure. Finally, the laser spallation technique requires much simpler post-experimental analysis than the standard techniques in arriving at the desired stress. Unlike the others where the evaluation of the local stresses is often complicated by non-uniform and plastic loading, the samples in the spallation technique are all loaded uniformly, uni-directionally and elastically. This advantage is however offset by the sophisticated instrumentation and the high cost of the hardware needed in setting up the laser spallation experiment.

ACKNOWLEDGEMENTS

This work was funded by the National Science Foundation Grant no. CMS 9696096 and Air Force Office of Scientific Research grant no. F49620-95-1-0242 for which the authors are grateful to Drs O. Dillon, W. Spitzig and W. Jones of these agencies.

REFERENCES

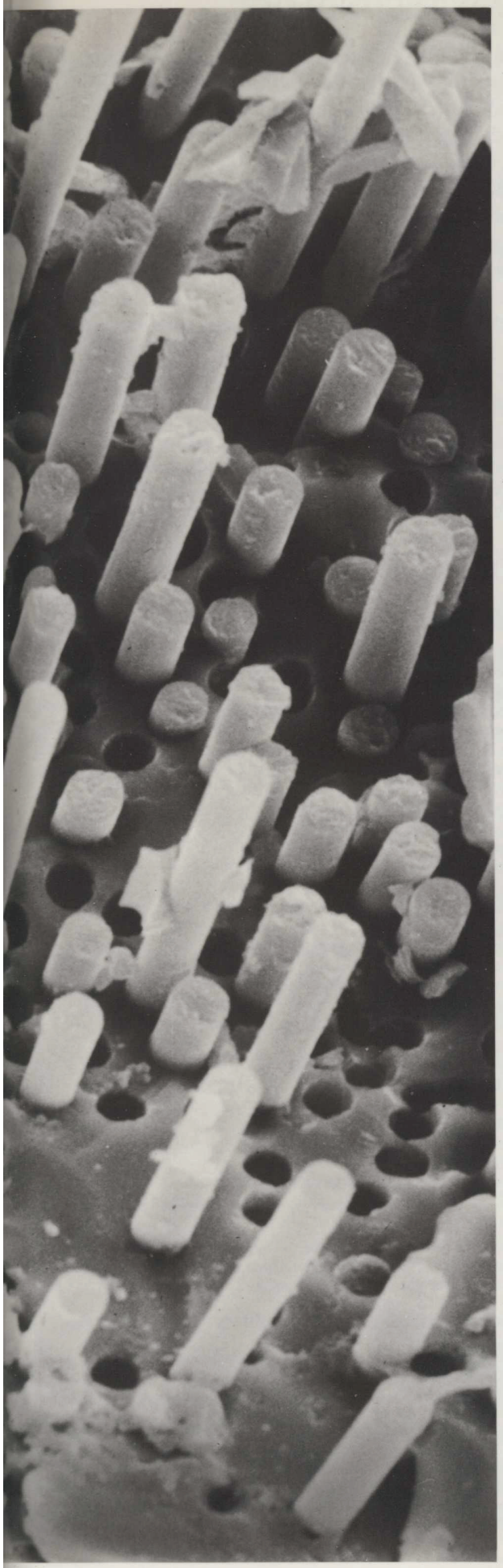
1. Gupta, V. and Pronin, A., A new technique to measure the toughness of thin-film interfaces. *J. Am. Ceram. Soc.*, 1995, **78**(5), 1397–4000.
2. Bagchi, A., Lucas, G. E., Suo, Z. and Evans, A. G., A new procedure for measuring the decohesion energy for thin ductile films on substrates. *J. Mater. Res.*, 1994, **9**(7), 1734–1741.
3. Gupta, V., Yuan, J. and Pronin, A., Recent developments in the laser spallation technique to measure the interface strength and its relationship to interface toughness with applications to metal/ceramic, ceramic/ceramic and ceramic/polymer interfaces. *J. Adhesion Sci. Technology*, 1994, **8**(6), 712–747.
4. Gupta, V., Argon, A. S., Parks, D. M. and Cornie, J. A., Measurement of interface strength by a laser spallation technique. *J. Mech. Phys. Solids*, 1992, **40**(1), 141–180.
5. Gupta, V. and Yuan, J., Measurement of interface strength by the modified laser spallation technique. II Applications to metal/ceramic interfaces. *J. Appl. Phys.*, 1993, **74**(4), 2397–2404.
6. Gupta, V. and Tian, X., Measurement of cleavage strength in ice crystals by a laser spallation technique. *J. Offshore Mechanics and Arctic Engineering*, 1994, **116**, 35–42.
7. Gupta, V., Argon, A. S., Cornie, J. A. and Parks, D. M., Measurement of interface strength by a laser-pulse-induced spallation. *Mater. Sci. Eng.*, 1990, **A126**, 105–117.
8. Miller, B., Muri, P. and Rebenfeld, L., A microbond method for determination of the shear strength of a fiber/resin interface. *Compos. Sci. Technol.*, 1987, **28**, 17–32.
9. Kelly, A. and Tyson, W. R., Tensile properties of fiber-reinforced metals: copper/tungsten and copper/molybdenum. *J. Mech. Phys. Solids*, 1965, **13**, 329–350.
10. Mandell, J. F., Grande, D. H., Tsiang, T. H. and McGarry, F. J., Composite materials: testing and design, *ASTM STP 327*, ASTM, 1986, p. 87.
11. Herrera-Franco, P. J. and Drzal, L. T., Comparison of methods for the measurement of fibre/matrix adhesion in composites. *Composites*, 1992, **23**(1), 2–26.
12. Yuan, J. and Gupta, V., The effect of microstructure and chemistry on the tensile strength of Nb/sapphire interfaces with and without interlayers of Sb and Cr. *Acta Metall. Mater.*, 1995, **43**(2), 781–794.
13. Gupta, V., Pronin, A. and Anand, K., Mechanisms and quantification of spalling failure in laminated composites under shock loading. *J. Compos. Mater.*, 1996, **30**(6), 722–747.
14. Barker, L. M. and Hollenbach, R. E., Laser interferometer for measuring high velocities of any reflecting surface. *J. Appl. Phys.*, 1972, **43**(11), 4669–4675.
15. Amery, B., Wide range velocity interferometer, *Sixth Symposium on Detonation*, Arlington, Virginia, 1976, pp. 673-681.
16. Adams, D. F. and Tsai, S. W., The influence of random filament packing on the transverse stiffness of unidirectional composites. *J. Compos. Mater.*, 1969, **3**, 308–318.
17. Mal, A., Bar-Cohen, Y. and Lih, S., Wave attenuation in fiber-reinforced composites. In *M^3D: Mechanics and Mechanisms of Material Damping, ASTM STP 1169*, eds V. K. Kinra and A. Wolfenden. American Society for Testing and Materials, Philadelphia, 1992, pp. 245–261.
18. King, T. R., Blackketter, D. M. and Adams, D. F., Micromechanics prediction of the shear strength of carbon fiber/epoxy matrix composites: the influence of the matrix and interface strengths. *J. Compos. Mater.*, 1992, **26**(4), 558–573.
19. Jungki, L. and Mal, A., A volume integral equation technique for multiple inclusion and crack interaction problems. *J. Appl. Mech.*, 1997, **64**(1), 23–31.
20. Blackketter, D. M., Upadhyaya, D. and King, T. R., Micromechanics prediction of the transverse tensile strength of carbon fiber/epoxy composites—the influence of the matrix and interface. *Polymer Composites*, 1993, **14**(5), 437–446.
21. *Ansys, Engineering Analysis System, Swanson Analysis Systems, Inc.*, Houston, Pennsylvania, 5.2 edition.
22. Crasto, A. S. and Kim, R. Y., On the determination of residual stresses in fiber-reinforced thermoset composites. *J. Reinforced Plastics and Composites*, 1993, **12**(5), 545–558.
23. Adams, D. F. and Miller, A. K., Hygrothermal microstresses in a unidirectional composite exhibiting inelastic material behaviour. *J. Compos. Mater.*, 1977, **11**, 285–299.
24. Yates, B., McCalla, B. A., Phillips, L. N. and Kingston-Lee, D. M., The thermal expansion of fibre-reinforced

Boeing Ex. 1032, p. 10 of 15
Boeing v. Regents Univ. Cal.

plastics. Part 5. the influence of matrix curing characteristics. *J. Mater. Sci.*, 1979, **14**, 1207–1217.
25. Hahn, H. T. and Pagano, N. J., Curing stresses in composite laminates. *J. Compos. Mater.*, 1975, **9**, 91–106.
26. Hofer, K. E., Rao, N., Jr and Laresen, D., Development of engineering data on the mechanical and physical properties of advanced composite materials—Part II, *Air Force Materials Laboratory-Technical Reports-72-205*, 1974.
27. Pagano, N. J. and Hahn, H. T., Evaluation of Composite Curing Stresses, Composite Materials: Testing and Design (Fourth Conference), *ASTM STP 617*, 1977, pp. 317–329.
28. Kaminski, B. E., Lemon, G. H. and McKague, E. L., Development of engineering data for advanced composite materials. Air Force Materials Laboratory-Technical Reports-70-108, **1**, 1972.
29. Oakeshott, J. L. and Fletcher, A. J., Thermal residual microstress generation during the processing of unidirectional carbon fibre/epoxy resin composites—regular fibre arrays. *Proceedings of the International Conference on Residual Stresses, Baltimore, MD*, 1994, pp. 569–578.
30. King, T. R., Blackketter, D. M. and Adams, D. F., Micromechanics prediction of the shear strength of carbon fiber/epoxy matrix composites: the influence of the matrix and interface strengths. *J. Compos. Mater.*, 1992, **26**(4), 558–573.

Boeing Ex. 1032, p. 11 of 15
Boeing v. Regents Univ. Cal.

VOL. 58 NO. 11 (1998)
ISSN 0266-3538



COMPOSITES SCIENCE AND TECHNOLOGY

Editor-in-Chief
Bryan Harris

North American Editor
Tsu-Wei Chou

Asian and Australasian Editor
Yiu-Wing Mai

Special Issue

MICROMECHANICS OF FIBRE-REINFORCED COMPOSITES

ELSEVIER

Boeing Ex. 1032, p. 12 of 15
Boeing v. Regents Univ. Cal.

COMPOSITES SCIENCE AND TECHNOLOGY

Composite materials offer lively new solutions to important engineering problems and exciting challenges to the designer who seeks to exploit their potential. In the competition with conventional engineering materials, the development of safe and economic applications for composites requires scientific understanding of their behaviour, rigorous modelling of complex stress analytical problems, and innovative approaches to manufacturing.

The journal *Composites Science and Technology* publishes refereed original articles, occasional review papers, and letters, on all aspects of the fundamental and applied science of engineering composites. It deals with fibre and particulate composites, with reinforced metals, plastics and ceramics, including cementitious materials, and natural composites like wood and bone. The editors welcome theoretical and experimental papers dealing with rheological, mechanical, chemical and physical properties, fatigue, fracture toughness, creep, durability and environmental effects, and papers on manufacture and design for specific purposes.

The journal particularly encourages an interdisciplinary approach to the study of composites, with a balanced experimental and analytical view of their behaviour.

Editor-in-Chief

PROFESSOR BRYAN HARRIS

Department of Materials Science
and Engineering,
University of Bath,
Claverton Down,
Bath BA2 7AY, UK
Fax: +44 (0) 1225 826098
E-mail: b.harris@bath.ac.uk

North American Editor

PROFESSOR TSU-WEI CHOU

Center for Composite Materials and Department
of Mechanical Engineering,
University of Delaware,
Newark, Delaware 19716, USA
Fax: +1 302 831 3619
E-mail: chou@me.udel.edu

Asian and Australasian Editor

PROFESSOR YIU-WING MAI

Centre for Advanced Materials Technology
Department of Mechanical and Mechatronic
Engineering
University of Sydney
Sydney, New South Wales 2006, Australia
Fax: +61 2 351 3760
E-mail: mai@mech.eng.usyd.edu.au

Editorial Board

L. A. Berglund
Luleå University of Technology, Sweden

W. J. Cantwell
University of Liverpool, UK

F.-K. Chang
Stanford University, California, USA

T. W. Clyne
University of Cambridge, UK

K. Friedrich
University of Kaiserslautern, Germany

H. Fukuda
Science University of Tokyo, Japan

T. Ishikawa
National Aerospace Laboratory, Tokyo, Japan

K. Kageyama
University of Tokyo, Japan

A. Kelly
University of Cambridge, UK

P. Ladevèze
Université de Paris VI, France

W. I. Lee
Seoul National University, South Korea

H. Lilholt
Risø National Laboratory, Roskilde, Denmark

A. C. Loos
Virginia Polytechnic Institute & State University, USA

T. X. Mao
Institute of Mechanics Academia Sinica, Beijing, China

S. T. Mileiko
Institute of Solid State Physics, Moscow, Russia

R. Naslain
Laboratoire des Composites Thermostructuraux, Pessac, France

R. E. Newnham
The Pennsylvania State University, USA

L. Nicolais
Universitá Degli Studi di Napoli, Italy

N. J. Pagano
Wright-Patterson Air Force Base, Ohio, USA

D. Perreux
LMARC Université de Franche Comté, Besançon, France

D. C. Phillips
Kobe Steel Europe Ltd, Guildford, UK

S. L. Phoenix
Cornell University, New York, USA

K. Schulte
Technical University Hamburg-Harburg, Hamburg, Germany

C. T. Sun
Purdue University, West Lafayette, Indiana, USA

H. D. Wagner
The Weizmann Institute of Science, Rehovot, Israel

M. R. Wisnom
University of Bristol, UK

R.-J. Wu
Shanghai Jiaotong University, China

A.-H. Zureick
Georgia Institute of Technology, USA

SUBSCRIPTIONS

1998—One volume, twelve issues per volume (Volume 58). Annual Institutional Subscription Rates 1998: Europe, The CIS and Japan 3749 Dutch Guilders. All other countries US$2155. Dutch Guilder prices exclude VAT. Non-VAT registered customers in the European Commmunity will be charged the appropriate VAT in addition to the price listed. Prices include postage and insurance and are subject to change without notice.

Any enquiries relating to subscriptions should be sent to:

The Americas: Elsevier Science Customer Support Department, PO Box 945, New York, NY 10010, USA (Tel: (+1) 212-633-3730/1-8888 4ES-INFO: Fax: (+1) 212-633-3680; e-mail: usinfo-f@elsevier.com).

Japan: Elsevier Science Customer Support Department, 9–15 Higashi-Azabu 1-chome, Minato-ku, Tokyo 106, Japan (Tel: (+3) 5561-5033: Fax: (+3) 5561-5047; e-mail: info@elsevier.co.jp).

Asia Pacific (*excluding Japan*): Elsevier Science (Singapore) Pte Ltd, No. 1 Temasek Avenue, 17-01 Millenia Tower, Singapore 039192 (Tel: (+65) 434-3727; Fax: (+65) 337-2230; e-mail: asianfo@elsevier.com.sg).

Rest of the World: Elsevier Science Customer Service Department, PO Box 211, 1001 AE Amsterdam, The Netherlands (Tel: (+31) 20-485-3757: Fax: (+31) 20-485-3432; e-mail: nlinfo@elsevier.nl).

Periodicals postage paid at Rahway, NJ and additional entry points. *Composites Science and Technology* (ISSN 0266-3538) is published one issue per month, January to December, in one volume by Elsevier Science Ltd, The Boulevard, Langford Lane, Kidlington, Oxford OX5 1GB, UK. The annual subscription in the USA is $2155. *Composites Science and Technology* is distributed by Mercury Airfreight International Ltd, 365 Blair Road, Avenel, NJ 07001, USA. Postmaster: please send address corrections to *Composites Science and Technology*, c/o Elsevier Science Regional Sales Office, Customer Support Department, 655 Avenue of the Americas, NY 10010, USA.

Boeing Ex. 1032, p. 13 of 15
Boeing v. Regents Univ. Cal.

COMPOSITES SCIENCE AND TECHNOLOGY

VOL. 58 1998

NOVEMBER

SPECIAL ISSUE

MICROMECHANICS OF FIBRE-REINFORCED COMPOSITES

Guest Editor

N. J. PAGANO

Editor-in-Chief

BRYAN HARRIS

North American Editor

TSU-WEI CHOU

Asian and Australasian Editor

YIU-WING MAI

DEC 16 1998

LIBRARY

ELSEVIER

Boeing Ex. 1032, p. 14 of 15
Boeing v. Regents Univ. Cal.

Copyright © 1998 Elsevier Science Ltd. All rights reserved.

This journal and the individual contributions contained in it are protected under copyright by Elsevier Scien Ltd, and the following terms and conditions apply to their use:

Photocopying

Single photocopies of single articles may be made for personal use as allowed by national copyright law Permission of the publisher and payment of a fee is required for all other photocopying, including multiple systematic copying, copying for advertising or promotional purposes, resale, and all forms of document deliver Special rates are available for educational institutions that wish to make photocopies for non-profit education classroom use.

Permissions may be sought directly from Elsevier Science Rights & Permissions Department, PO Box 80 Oxford OX5 1DX, UK; phone: (+44) 1865 843830, fax: (+44) 1865 853333, e-mail: permissions@elsevier.co.u You may also contact Rights & Permissions directly through Elsevier's home page (http://www.elsevier.nl selecting first 'Customer Support', then 'General Information', then 'Permissions Query Form'.

In the USA, users may clear permissions and make payment through the Copyright Clearance Center, Inc., 22 Rosewood Drive, Danvers, MA 01923, USA; phone: (978) 7508400, fax: (978) 7504744, and in the UK through th Copyright Licensing Agency Rapid Clearance Service (CLARCS), 90 Tottenham Court Road, London W1P 0LI UK; phone: (+44) 171 436 5931; fax: (+44) 171 436 3986. Other countries may have a local reprographic right agency for payments.

Derivative Works

Subscribers may reproduce tables of contents or prepare lists of articles including abstracts for internal circulatio within their institutions. Permission of the publisher is required for resale or distribution outside the institution.

Permission of the publisher is required for all other derivative works, including compilations and translations.

Electronic Storage or Usage

Permission of the publisher is required to store or use electronically any material contained in this journal including any article or part of an article. Contact the publisher at the address indicated.

Except as outlined above, no part of this publication may be reproduced, stored in a retrieval system or trans mitted in any form or by any means, electronic, mechanical, photocopying, recording or otherwise, without prio written permission of the publisher.

Address permissions requests to: Elsevier Science Rights & Permissions Department, at the mail, fax and e-mai addresses noted above.

Notice

No responsibility is assumed by the publisher for any injury and/or damage to persons or property as a matter o products liability, negligence or otherwise, or from any use or operation of any methods, products, instructions o ideas contained in the material herein. Because of rapid advances in the medical sciences, in particular, independen verification of diagnoses and drug dosages should be made

Although all advertising material is expected to conform to ethical (medical) standards, inclusion in this publicatio does not constitute a guarantee or endorsement of the quality or value of such product or of the claims made of i by its manufacturer.

The Item-fee Code for this publication is: 0266-3538/98

Back Issues: Back issues of all previously published volumes are available direct from Elsevier Science Office (Oxford and New York). Complete volumes and single issues can be purchased for 1990–1997. Earlier issues are available in high quality photo-duplicated copies as complete volumes only. Back volumes on microfilm are available from UMI, 300 North Zeeb Road, Ann Arbor, MI 48106, USA.



ContentsDirect, the ***free*** e-mail alerting service, delivers the table of contents of this journal directly to your PC, prior to publication. The quickest way to register for **ContentsDirect** is via the Internet at: **http://www.elsevier.nl/locate/ContentsDirect**. If you don't have access to the Internet you can register for this service by sending an e-mail message to cdsubs@elsevier.co.uk —specifying the title of the publication you wish to register for.

Printed in Great Britain by Alden Press, Oxford

Boeing Ex. 1032, p. 15 of 15
Boeing v. Regents Univ. Cal.